J Therm Anal Calorim
DOI 10.1007/s10973-012-2559-0

TG–DSC–FTIR–MS study of gaseous compounds evolved during thermal decomposition of styrene-butadiene rubber

Antonyraj Arockiasamy · Hossein Toghiani · David Oglesby · M. F. Horstemeyer · J. L. Bouvard · Roger L. King

Received: 28 October 2011 / Accepted: 15 June 2012

Abstract The thermal decomposition behavior of styrene-butadiene rubber was studied using a system equipped with thermogravimetric analysis, differential thermal analysis, Fourier transform infrared spectroscopy, and mass spectroscopy. Two different experiments were conducted. From these experiments, thermogravimetric analysis results indicated a mass loss of 58 % in the temperature range of ~290–480 °C and a mass loss of 39 % in the temperature range beyond 600 °C. Scanning electron microscopy coupled with energy-dispersive X-ray spectroscopy confirmed the presence of oxides, even at 1,000 °C, accounting for the Zn, Mg, Al, Si, and Ca in the original sample.

Keywords Thermal analytical techniques · Styrene-butadiene rubber · Compositional analysis

Introduction

The demand for rubber products in the automotive and aerospace industries is continually increasing due to their desirable properties including flexibility, elasticity, restorability, impermeability, resistivity, and non-reactivity toward alkalis, acids, and oil [1]. A variety of reinforcing fillers, antioxidants, antidegradants, and plasticizers, including carbon black and hydrocarbon oil, are added to improve the inherent physicochemical properties of the rubber. These additives result in augmented strength, extended lifetime, improved oxidation resistance, aging, diffusion, thermal stability, and flammability [2]. Efforts continue in this area [3, 4]. A combination of pyrolysis-gas chromatography (Py-GC) and pyrolysis-gas chromatography/mass spectrometry (Py-GC/MS) has evolved as the primary method to elucidate the chemical composition of rubbers [5–14]. In particular, Ghebremeskel and coworkers [12] quantified the styrene content of SBR copolymers using Py-GC/MS. Lee and coworkers [15] studied the composition of a natural rubber/SBR/butyl rubber ternary blend system using thermal analytical tools (TG), DTA, FTIR, and Py-GC/MS. Currently, the combination of these thermal techniques (TG–DSC–FTIR–MS) is considered as a powerful tool for evaluating a material's characteristics including its thermal stability, decomposition kinetics, and life expectancy. With this tool, the substance of interest is observed during exposure to predefined temporal variations in temperature, and a physical property (mass and enthalpy) is measured as the response. Choudhury et al. and coworkers [16] recently reviewed the thermal characterization of the elastomeric materials using different thermoanalytical techniques, including the methods of TG, differential scanning calorimetry (DSC), DTA, dynamic mechanical analysis (DMA), combined TG–DSC, TG–DTA, and simultaneous TG–FTIR and TG–MS techniques. Among the thermal methods, thermogravimetric analysis quantifies the mass/change of mass due to different processes including outgassing, dehydration, devolatilization,

A. Arockiasamy (✉)
Environmental Health and Safety, The University of Mississippi Medical Center, 2500 North State Street, Jackson, MS 39216, USA
e-mail: aarockiasamy@umc.edu

A. Arockiasamy · D. Oglesby · M. F. Horstemeyer · J. L. Bouvard · R. L. King
Center for Advanced Vehicular Systems, Mississippi State University, 200 Research Boulevard, Starkville, MS 39759, USA

H. Toghiani
Dave C. Swalm School of Chemical Engineering, Mississippi State University, Mississippi State, MS 39762, USA

Published online: 25 July 2012

decomposition, oxidation, reduction, and other chemical reactions as a function of temperature and/or time. Differential scanning calorimetry examined the heat evolution from/absorption by a sample in a controlled environment and provides information regarding phase transitions, chemical reactions, precipitation, and dissolution [17, 18]. FTIR is a non-destructive method that allows the identification of chemical composition and/or bonding present in an unknown molecule. MS provides information regarding the number and type of fragment ions liberated when a molecule is dissociated; each molecule gives rise to a particular combination of fragment ions.

In the present study, the gases evolved during thermal decomposition of rubber under a nitrogen atmosphere and thermal oxidation under an air atmosphere were examined. A combination of TG–DSC–FTIR–MS was used to quantify the evolved gases from rubber. The testing methodology employed in this work fully adhered to the ASTM methods [20–25].

Experimental

The rubber used in road wheel backer pads mainly consists of SBR along with reinforcing fillers, antiozonants, and antidegradants. Our recent publication regarding the mechanical behavior and fatigue studies of this classical rubber component is presented in ref. [1]. Scanning electron microscopy (SEM) coupled with energy-dispersive X-ray spectroscopy (EDS) were used to examine the morphology of rubber (shape and diameter), the distribution of reinforcing fillers and to quantify the elemental composition of oxides present in the rubber.

A specimen with a height of approximately 20 mm and a thickness of $\sim$3 mm was cut with a specially designed razor blade holder (holder designed in-house). The specimen was examined for microstructural changes. Polymer specimens are typically prepared with three factors taken into account to obtain the best microstructure analysis: (a) isolation of the sample surface; (b) enhancement of contrast; and (c) minimization of radiation damage to the sample. These factors must be considered due to the poor conductivity of most elastomers combined with the low-energy density of X-rays [26]. Samples were sputter coated with platinum and palladium/gold for a period of 10–20 min to improve their conductivity, enhance the contrast, and minimize the radiation effects on specimens [26]. Different methods have been employed to enhance the contrast in images of elastomeric materials. These methods include staining, etching, replication, shadowing, and metal decoration [27–32]. In this work, a 2 % osmium tetroxide (OsO_4) solution was employed as a staining agent. The rubber sample was stained for a period of 24 h, and then air dried. The main function of OsO_4 is to react

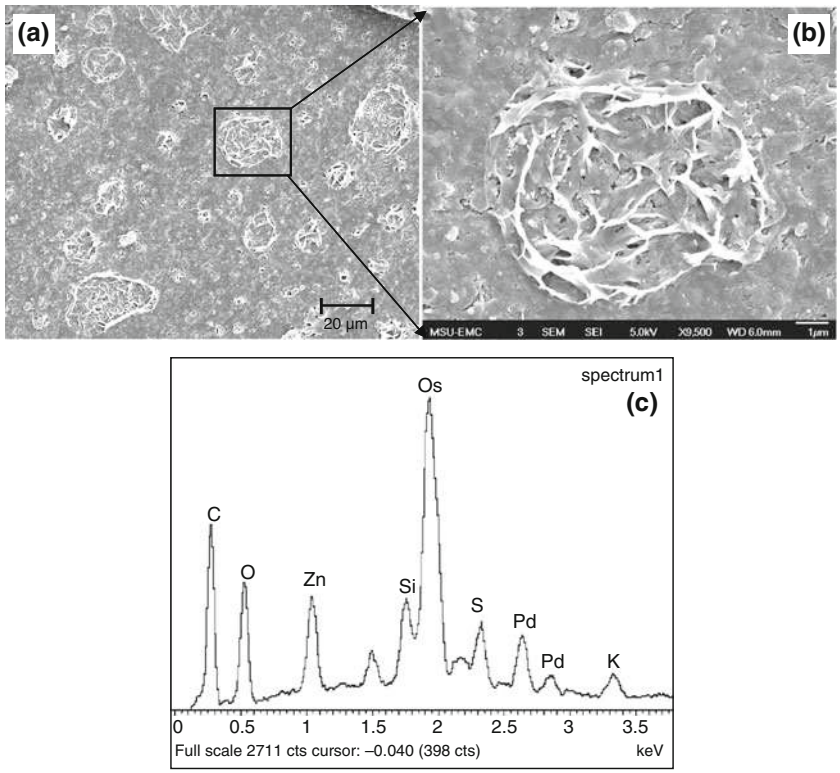

Fig. 1 **a** Morphology of OsO_4 deposit on rubber and its EDX spectrum in (**c**). A magnified image is shown in Fig. 1b

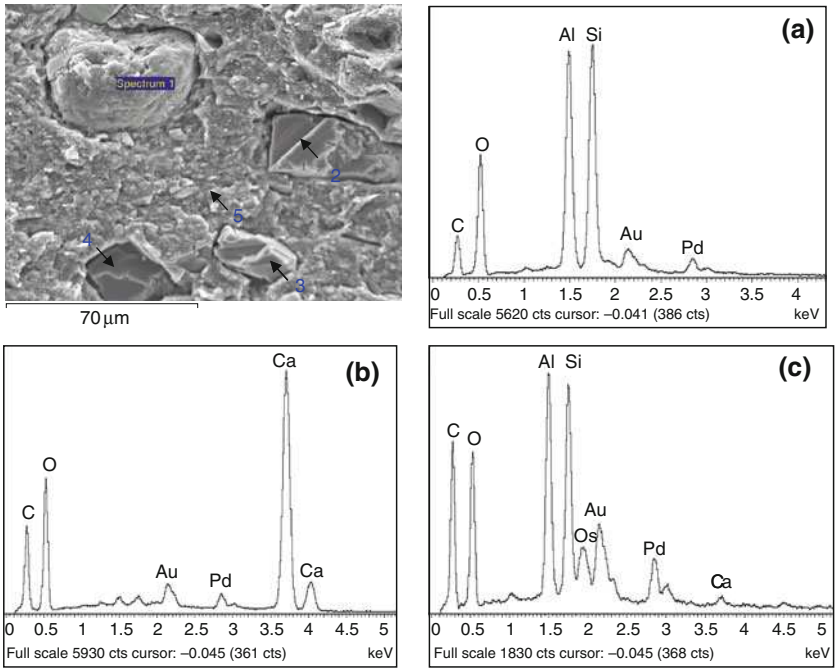

Fig. 2 SEM images of thin cross section of SBR. EDX spectra show the regions where silicon, aluminum, calcium, and their oxides exist

with any carbon–carbon double bonds in the unsaturated rubber, staining the rubber through generation of an osnate ester, which is responsible for the excellent contrast [33]. An illustrative chemical reaction that takes place on elastomers containing carbon–carbon double bonds is given in ref. [33]. When treated with OsO_4, the double bond in butadiene reacts preferentially, bonding with the oxide. The presence of a heavy metal is sufficient to block the electron beam, so the polystyrene domains are seen clearly in the SEM. SEM images exploring the morphology of OsO_4, stained on SBR are shown in Fig. 1a and magnified in Fig. 1b. Figure 1c is an EDX spectrum of OsO_4.

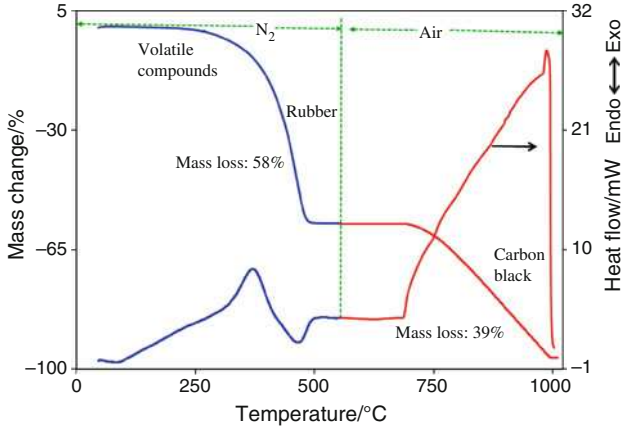

Fig. 3 TG–DTG plot of SBR rubber tested at a heating rate of 10 °C min^{-1} in N_2 atmosphere up to 550 °C and then changed to air up to 1,000 °C

Thermogravimetric and differential thermal analyses (TG–DSC)

TG–DSC analysis was performed using the LabSys Setaram (Setaram Instrumentation, Inc.) The rubber was cut into thin sections of ~20–30 mg using a razor blade. In the first study, a thermal decomposition experiment was carried out over the temperature range of 50–850 °C, with a heating rate of 10 °C min^{-1}, under a nitrogen atmosphere (flow rate of 75 cm^3 min^{-1}). In the second study, a thermal decomposition/oxidation experiment was carried out over the temperature range of 50–1,000 °C with a heating rate of 10 °C min^{-1}. In this experiment, the nitrogen flow was maintained until the temperature reached 550 °C. At this temperature, the nitrogen flow was switched off and air, at a flow rate of 75 cm^3 min^{-1}, was turned on and maintained while the temperature continued to increase at a rate of 10 °C min^{-1} until 1,000 °C. Thermal response curves in the form of mass change and heat flow as a function of temperature and time were recorded using the SetSys software (V 4.3). In this software, the derivative of the primary mass change (DTG) was utilized, thereby extended the capability and scope of the analysis. Using this procedure, the percent mass of total organic compounds, carbon black, and ash in rubber was determined.

Mass spectra analysis (MS)

The mass spectra analysis was carried out using a Pfeiffer Instruments Quadruple Mass Spectrometer, operating at 90 eV ionization energy. The evolved gases during thermal

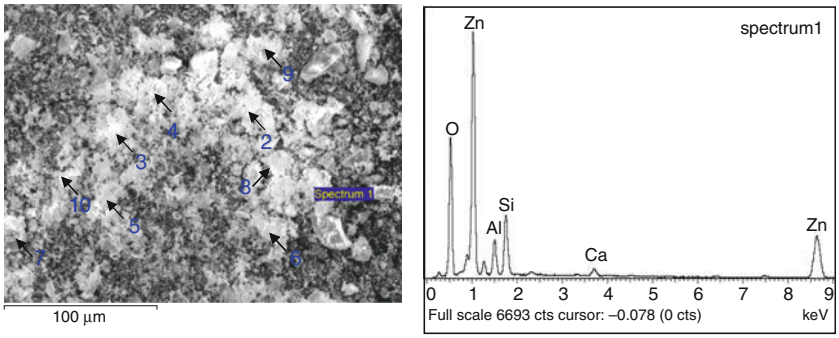

Fig. 4 SEM–EDX Spectrum of the residue obtained from the rubber

Table 1 EDX elemental analysis for tire residue at different locations after thermal treatment

Location	Element/wt.%				
	Zn	Mg	Al	Si	Ca
1	72.8	6.7	11.8	19.9	2.0
2	90.9	4.9	4.1	10.4	1.1
3	86.1	3.7	2.8	7.9	3.2
4	78.4	6.1	7.5	18.7	1.8
5	47.0	18.9	1.6	41.6	10.8
6	85.7	8.0	9.6	15.8	1.4
7	47.7	10.1	9.3	44.6	6.0
8	81.9	6.2	5.9	19.3	1.4
9	77.9	8.2	6.5	29.1	1.3
10	59.3	5.9	12.7	29.5	1.4

decomposition experiments were directly transferred by means of a capillary column transfer line (heated to 150 °C) and detected by the mass spectrometer. The possible species liberated from rubber during a thermal decomposition process are hydrogen ($H_2 = 2$), methane ($CH_4 = 16$), water ($H_2O = 18$), carbon monoxide ($CO = 28$) or ethylene ($C_2H_4 = 28$), oxygen ($O_2 = 32$), carbon dioxide ($CO_2 = 44$), butane ($C_4H_{10} = 58$), benzene ($C_6H_6 = 78$), toluene ($C_7H_8 = 92$), ethyl benzene ($C_6H_5H_2CH_3 = 106$), ethyl cyclohexane ($C_8H_{16} = 112$), styrene ($C_8H_8 = 104$), 1-methyl -4 (1-methyl ethyl benzene) ($C_{10}H_{14} = 134$), and limonene ($C_{10}H_{16} = 136$). Using this list of species, the MS method was established to identify the mass fragments of their respective ions produced in the positive mode of ionization.

The standard Blazers software (Quardstar®) was used for rapid control of the MS instrument settings, real-time data collection, and post-acquisition processing. All spectral information was displayed on the screen during the run, and mass-specific curves were plotted as chemo-selective records as the gases were evolving. The major components evolving over the temperature cycle were monitored in the selected multiple ion mode (intensity vs. time).

Fourier transform infrared spectroscopy (FTIR)

FTIR spectra were recorded on a Thermo Corporation FTIR spectrometer operating in absorption mode over the frequency range of 4,000–400 cm^{-1}. The evolved gases from TG were analyzed by collecting and averaging 64 scans with a resolution of 4 cm^{-1}. The temperature of the transfer line was maintained at 200 °C.

Results and discussion

The morphology of a thin cross section of rubber is shown in Fig. 2. Also shown are corresponding EDX spectra, confirming the presence of additives. The particles ranged in size from 15 to 60 µm, and are surrounded by the SBR matrix. The large agglomerated particles shown are of

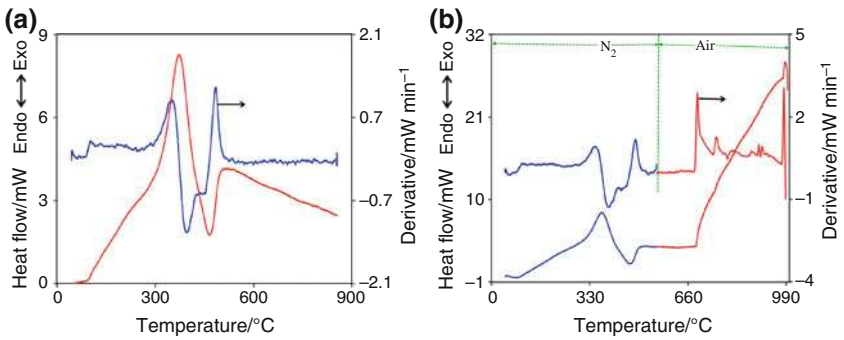

Fig. 5 DSC and its derivative plot of rubber tested at a heating rate of 10 °C min^{-1} in **a** N_2 atmosphere up to 850 °C and **b** N_2 atmosphere up to 550 °C and then changed to an air atmosphere up to 1,000 °C

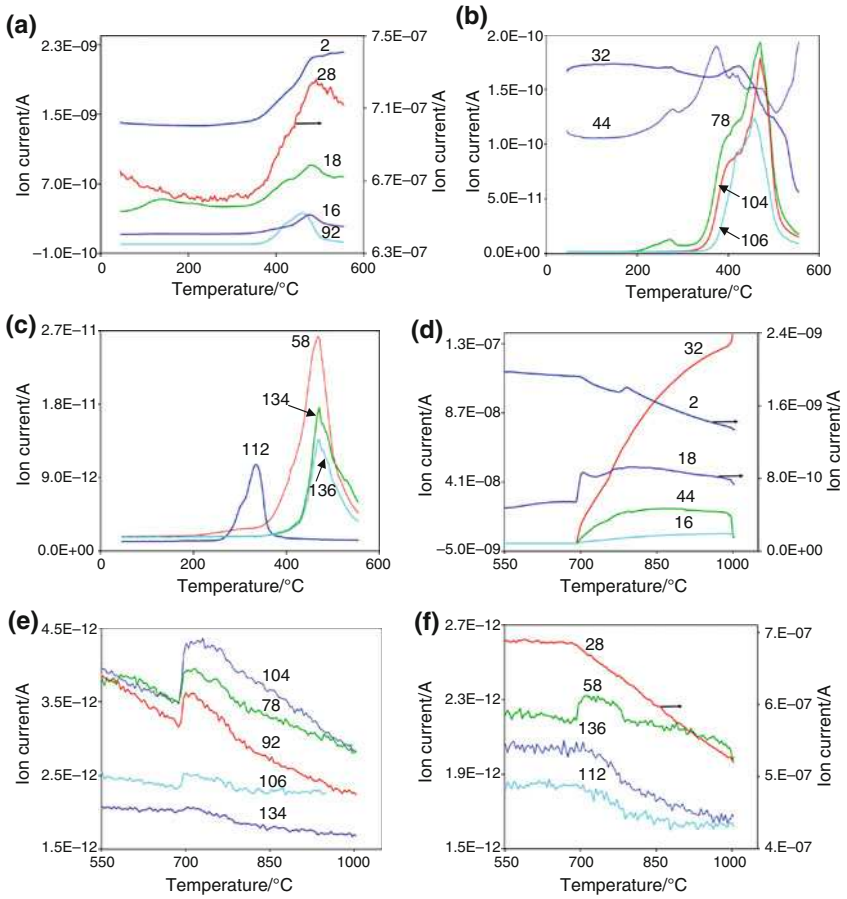

Fig. 6 Ion currents of selected ions to represent the mainly released chemical species during rubber pyrolysis. **a–c** heating segment in the temperature range of 50–550 °C and **d–f** heating segment in the temperature range of 550–1,000 °C

aluminosilicate clay, (Fig. 2a in location 1), calcium carbonate in locations 2–4 (spectrum in Fig. 2b), and a combination of both in location 5 (spectrum in Fig. 2c).

A representative TG-DTG curve for SBR is shown in Fig. 3 for the test carried out in ultrahigh purity nitrogen up to 550 °C and then changed to air up to 1,000 °C. In this figure, a sharp decline in mass starting at a temperature of 288 °C was observed with the decline ending at 480 °C. This plateau region corresponds to a mass loss of 58 % under the nitrogen environment. This mass loss is representative of the amount of noncarbon black organic additives including oil and plasticizer.

When the test was carried out in air (switched from nitrogen at 550 °C), a second plateau region was evident spanning the temperature range of 670–985 °C. This mass loss constitutes an additional 39 %. This mass loss is representative of the amount of carbon content (carbon black). The carbon is converted to carbon monoxide and carbon dioxide during the oxidation process. The remaining residue (985–1,000 °C) constitutes 3 % of the mass, and corresponds to the ash content/nonvolatile additives (oxides of Zn, Al, Ca, Mg, Si, etc.). Analysis of ash content using energy-dispersive X-ray analysis (EDX) in ten different locations confirmed the presence of these elements in the residue. Figure 4 shows the SEM micrograph and the EDX spectra for the ash, while Table 1 provides a compilation of the wt% distribution of the targeted elements (Zn, Mg, Al, Si, Ca). The Zn is the dominant element presents (average ~75 %), while Si, Mg, Al, and Ca are present in decreasing amounts.

The calculation of ash content, R, and carbon content, C, from a dry sample was performed according to ASTM methods [22, 25]. Equations for these calculations are shown as Eqs. (1) and (2):

$$R = [(F - E)/(D - E)] \times 100 \quad (1)$$

$$C = 100\,(Q - F)/(D - E)(1 - 0.01R), \quad (2)$$

where F is the mass of crucible plus ash after oxidation of the carbon black, g; and E is the mass of crucible, g; D is the mass of original dry sample plus crucible, g; Q is the mass of crucible and residue after evolution of hydrocarbon, g.

The derivative curves DTG of both TG curves show a broad shoulder over the mass loss temperature ranges mentioned previously. Usually, this curve may be used to identify the type of elastomeric system. Natural rubber exhibits a peak maximum at ~365 °C while SBR-BR and BR exhibit a peak at ~450 °C [34].

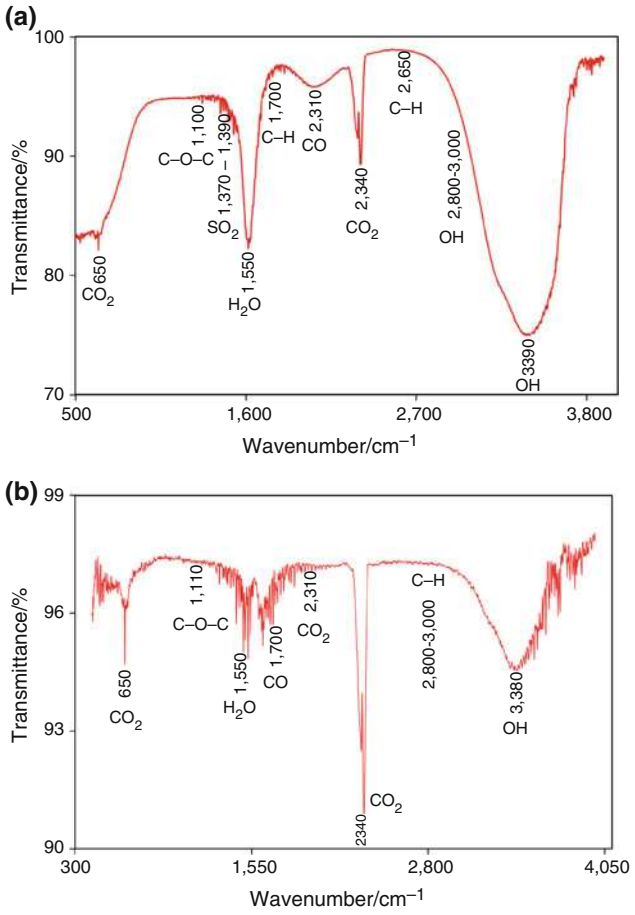

Fig. 7 FTIR spectrum of gases released by heating of rubber under a heating rate of 10 °C min^{-1} **a** in N_2 atmosphere up to a maximum temperature of 550 °C and **b** in an air atmosphere from 550 °C to 1,000 °C

The heat flow curves generated from DSC for the investigated rubber in nitrogen and air are shown in Fig. 5. Two exothermic peaks in the temperature range of 200–455 and 678–985 °C (Fig. 5a, b) are observed. These peaks show a peak maximum of 372 and 769 °C, respectively. One endothermic peak is observed in the temperature range of 372–490 °C with a peak maximum of 456 °C. These two exothermic peaks reveal the volatilization of highly volatile matter such as moisture, plasticizer, residual solvents, oils, or other low boiling (300 °C or less) components, and moderately volatile matter (including the rubber type). Once the organic compounds have been pyrolyzed, a plateau region is observed (around 550 °C). When the atmosphere was changed from nitrogen to air (Fig. 5b), the carbon black was oxidized, leaving the ash residue [34]. An endothermic peak appears with a peak maximum of 456 °C, corresponding to the melting of inorganic/organic additives or filler materials [16].

In Fig. 6, two prominent regions are clearly observed. The first region corresponds to the temperature span where organic additives are lost, between 200 and 485 °C. The second region corresponds to the temperature range where carbon black is oxidized, between 670 and 985 °C. In addition, the DSC curves exhibit two strong exothermic peaks, appearing in the temperature regions of 301–456 and 678–985 °C. These peaks confirm that there is volatilization (or evaporation) of noncarbon black organic additives and carbon black additives from the rubber.

In addition, it was assumed that there is a possibility of thermodynamically feasible oxidation and reduction reactions, and thermolytic cleavage of rubber, primarily consisting of an isoprene unit (2-methyl-1,3-butadiene) [36]. This isoprene unit is usually attached to different functional groups (methyl, ethyl, butadiene, styrene, etc.) depending upon the type of rubber. During the pyrolysis process, the isoprene unit and the functional groups attached to it will break into several fragments that may be detected by FTIR and MS [35]. Based on the thorough literature survey and ASTM methods, some of the possible species of these volatile compounds are hydrogen ($H_2 = 2$), methane ($CH_4 = 16$), water ($H_2O = 18$), carbon monoxide ($CO = 28$) or ethylene ($C_2H_4 = 28$), oxygen ($O_2 = 32$), carbon dioxide ($CO_2 = 44$), butane ($C_4H_{10} = 58$), benzene ($C_6H_6 = 78$), toluene ($C_7H_8 = 92$), ethyl benzene ($C_6H_5CH_2CH_3 = 106$), ethyl cyclohexane ($C_8H_{16} = 112$), styrene ($C_8H_8 = 104$), 1-methyl -4 (1-methyl ethyl benzene) ($C_{10}H_{14} = 134$), and limonene ($C_{10}H_{16} = 136$) [35–38]. The MS results of these fragments from evolved species during thermal decomposition (N_2 to 550 °C) and during thermal oxidation (air to 1,000 °C) are shown in Fig. 6.

Semi-quantitative evaluation of rubber

An effort to semi-quantitatively analyze the evolved gas composition yielded by decomposition/thermal oxidation of the rubber was undertaken. This attempt employed the "multiple ion detection" (MID) mode. In TG–MS analysis, the amount of sample used for the pure nitrogen experiment was 28 mg, and the residue remaining was 11.8 mg. The difference between these two values (16.2 mg) corresponds to the amount of evolved gas. Similarly, for the nitrogen/air experiment, the sample used was 31.6 mg, and the residue remaining was 0.7 mg. The difference between these values (30.9 mg) corresponds to the amount of evolved gas.

As previously shown in Fig. 6, the evolved species include hydrogen, methane, water, carbon monoxide, ethylene, oxygen, carbon dioxide, butane, benzene, toluene, ethyl benzene, ethyl cyclohexane, styrene, 1-methyl-4 (1-methyl ethyl benzene), and limonene. The amount, $A(j)$, of a given species, j, is calculated by integration of the species' representative m/z ion profile over the entire experiment. The result of this integration process, $Im/z(j)$, is then divided by the relative intensity, $r(j)$, that the ion

Table 2 Integrated ion current value of MS spectra and chemical composition of gas mixture

Chemical formula	Compounds name	Atomic mass	Heating in N_2 atm. till 550 °C		Mean ion current/A	Molar mass/%	Mass/%
			Onset/ °C	Peak/ °C			
H_2	Hydrogen	2	308	375	1.7E−09	2.4E−01	1.7E−02
CH_4	Methane	16	433	475	1.8E−09	2.6E−01	1.5E−01
H_2O	Water	18	431	475	5.9E−10	8.6E−02	5.5E−02
CO/C_2H_4	Carbon monoxide/ethylene	28	440	479	6.5E−07	9.4E+01	9.3E+01
O_2	Oxygen	32	418	525	3.4E−08	4.9E+00	5.6E+00
CO_2	Carbon dioxide	44	313	375	3.7E−09	5.4E−01	8.4E−01
C_4H_{10}	Butane	58	414	467	3.3E−12	4.8E−04	9.9E−04
C_6H_6	Benzene	78	350	471	1.5E−11	2.2E−03	6.1E−03
C_7H_8	Toluene	92	393	458	2.1E−11	3.0E−03	9.8E−03
C_8H_{10}	Ethyl benzene	106	387	458	8.5E−12	1.2E−03	4.6E−03
C_8H_{16}	Ethyl cyclohexane	112	407	463	2.5E−12	3.6E−04	1.4E−03
C_8H_8	Styrene	104	424	471	1.2E−11	1.8E−03	6.5E−03
$C_{10}H_{14}$	1-methyl-4-(1-methyl ethyl benzene)	134	443	471	2.6E−12	3.8E−04	1.8E−03
$C_{10}H_{16}$	Limonene	136	440	471	2.3E−12	3.4E−04	1.6E−03

has in the mass spectrum of the pure substance, to obtain the amount of species j present, $A(j) = Im/z(j)/r(j)$. Table 2 summarizes (1) the relative intensity of each ion detected in the mass spectrum of each pure chemical species as recorded in TG–MS analyses $[r(i) = h(i)/\Sigma h(i)]$, where $h(i)$ represents the height of the m/z peak in the mass spectrum of that species; (2) the integrated values of the appropriate ion currents [I$m/z(i)$], subsequently employed in the data processing; (3) the calculated amount of each species. From the calculated values, $A(j)$, the molar mass percentage of each chemical species in the total evolved gas phase was calculated: $\%\text{mol}\ (j) = 100A(j)/\Sigma A(j)$. Subsequently, the absolute amount of each released species was evaluated (Table 2) from the total mass loss of the rubber sample [18.3 mg (58 %)]. Table 2 shows the semi-quantitative analysis of the gas phase.

FTIR analyses

Gaseous compounds that evolved during thermal decomposition in the temperature range of 50–550 and 550–1,000 °C were identified using the FTIR spectra shown in Fig. 7a and b. In Fig. 7a, the FTIR spectra appear as broad bands in the frequency ranges of 3700–2800, 2370–2230, 2180–1830, and 1750–1500 cm^{-1}, which correspond to the stretching/vibrational frequencies of O–H, C=O, C–O (C–C), and H–O–H, respectively. There is a signature representative of the formation and liberation of different organic compounds due to the presence the characteristic C–H bending vibration that appears at 1,340–1,480 cm^{-1}. Other characteristic peaks corresponding to methane (1,307 cm^{-1}) and ethane (1,457 cm^{-1}) are also observed. The presence of the C=O stretching vibration band appearing at 1,710–1,720 cm^{-1} and the C–OH stretching vibration band appearing at 1,075–1,000 cm^{-1} shows the formation and liberation of alcohol and ketone groups. The characteristic peaks for ethanol (1,244 and 1,052 cm^{-1}), sulfur dioxide emission at (1,376, and 1,361 cm^{-1}), and ethylene emission at 1,650 and 950 cm^{-1} were also observed in the FTIR spectra.

The FTIR spectra shown in Fig. 7b reveal the bands characteristic of more volatile species such as methane, ethane, ethylene, alcohols, and compounds with carbonyl groups as well as the absorption bands of CO_2 and H_2O. However, the absorption bands for water are less intense than the respective bands in the FTIR spectra shown in Fig. 7a. Similarly, the intensity of the CO_2 band in Fig. 7b is increased, but the intensity of the C–H bands are decreased.

Conclusions

Thermal decomposition and thermal oxidation of SBR rubber was examined with a focus on the composition of evolved gases during the thermal process. Using a suite of analytical tools (TG–DSC–FTIR–MS), species present in the evolved gas were identified, as were the relative amounts of noncarbon black organic additives, carbon black, and ash. SEM–EDX identified the large agglomerated particles of aluminosilicate, calcium carbonate, and a combination of both compounds in the rubber. The size of these particles was in the range of 15–60 μm in this particular type of SBR. In the decomposed final product (ash content), the amount of Zn was predominant along with trace amounts of Si, Mg, Al, and Ca.

Mass spectrometer analysis confirmed that ethylene and benzene were the primary decomposition products, on the

basis of ion fragments generated. Ethylene and benzene represented 87.9 and 5.7 % of the mass of gas evolved, respectively. FTIR results supported the presence of functional groups including OH, C–H, and C=C, C=O and O–C–O.

Acknowledgements This material is based upon work supported by the U.S. Army TACOM Life Cycle Command under Contract No. W56HZV-08-C-0236, through a subcontract with Mississippi State University, and was performed for the Simulation Based Reliability and Safety (SimBRS) research program. Any opinions, findings, conclusions, or recommendations expressed in this material are those of the author(s) and do not necessarily reflect the views of the U.S. Army TACOM Life Cycle Command. The authors would also like to acknowledge the support of the Center for Advanced Vehicular Systems (CAVS) at Mississippi State University (MSU).

References

1. Brown HR, Bouvard JL, Oglesby D, Marin E, Francis D, Antonyraj A, Toghiani H, Wang PT, Horstemeyer MF. Mechanical behavior and fatigue studies of rubber components used in tracked vehicles. http://www.dtic.mil/cgi-bin/GetTRDoc?Location=U2&doc=GetTRDoc.pdf&AD=ADA530663.
2. Rybinski P, Janowsk G, Kucharska J, Jastrzabek A. Influence of surface modification on thermal stability and flammability of cross-linked rubbers. J Therm Anal Calorim. 2010;100:1037–44.
3. Mati M, Mitra S, Bhowmiek AK. Effect of nanoclays on high and low temperature degradation of fluoroelastomers. Polym Degrad Stab. 2008;93:188–200.
4. Janowska T, Rybinski O, Jantas R. Effect of the modification of silica on thermal properties and flammability of cross-linked butadiene-acrylonitrile rubbers. J Therm Anal Calorim. 2007;87:511–7.
5. Radell EA, Strutz HC. Identification of acrylate and methacrylate polymers by gas chromatography. Anal Chem. 1959;31:1890–1.
6. Lehrle RS, Robb JC. Direct examination of the degradation of high polymers by gas chromatography. Nature. 1959;183:1671.
7. Hackathorn MJ, Brock MJ. Determination of head–head and tail–tail structures in polyisoprenes. Rubber Chem Technol. 1972;45:1295–302.
8. Lattimer RP, Harris RE, Rhee CK, Schulten HR. Identification of organic compounds in uncured rubber compounds using mass spectrometry. Rubber Chem Technol. 1988;61:639–57.
9. Schulten HR, Plage B, Lattimer RP. Pyrolysis-field ionization mass spectrometry of rubber vulcanizates. Rubber Chem Technol. 1989;62:698–708.
10. Bach J, Braun D, Mueller I, Wendorff JH. Aging of rubber modified thermoplastics and elastomers. Angew Makromol Chem. 1985;137:21–34.
11. Matheson MJ, Wampler TP, Simonsick WJ. The effect of carbon black filling on the pyrolysis behavior of natural and synthetic rubber. Rubber World. 1996;213:14–6.
12. Ghebremeskel GN, Sekinger JK, Hoffpauir JL, Hendrix C. A study of the thermal degradation products of styrene-butadiene type rubber by pyrolysis/GC/MS. Rubber Chem Technol. 1996;69:874–84.
13. Chien JCW, Kiang JKY. Polymer reactions. X. Thermal pyrolysis of poly(isoprene). Eur Polymer J. 1979;15:1059–65.
14. Wang J, Pan Y, Fang Y, Wang Y. Determination of the rubber composition in styrene–butadiene latex by pyrolysis gas chromatography. Huaxue Shijie. 1985;26:177–9.
15. Lee YS, Lee W, Cho S, Kim H. Quantitative analysis of unknown compositions in ternary polymer blends: a model study on NR/SBR/BR system. J Anal Appl Pyro. 2007;78:85–94.
16. Choudhury NR, De P, Dutta NK. Thermal analysis of rubbers and rubbery materials. U.K.: Smithers Rapra Technology Ltd.; 2010. p. 546.
17. Antonyraj A, German RM, Wang PT, Horstemeyer MF. DSC analysis of Al6061 aluminum alloy powder by rapid solidification: effect of additives. J Therm Anal Calorim. 2010;100:361–6.
18. Mullens J. EGA—evolved gas analysis. In: Brown ME, editor. Handbook of thermal analysis and calorimetry, vol 1, Chapter 12. Amsterdam: Elsevier Science; 1998. p. 1509–46.
19. Macaione DP, Sacher RE, Singler, RE. Thermogravimetric characterization of elastomers and carbon-filled rubber composites for military applications. ASTM special technical publication. Compos Anal Thermograv. 1988;99759–69.
20. ASTM D297-93 e2, Standard test methods for rubber products-chemical analysis; 2002.
21. ASTM E1131-98, Standard test method for compositional analysis by thermogravimetry; 2003.
22. ASTM D6370-99, Standard test method for rubber-compositional analysis by thermogravimetry; 2003.
23. ASTM D3677-00, Standard test methods for rubber-identification by infrared spectrophotometry; 2004.
24. ASTM E1641-07, Standard test method for decomposition kinetics by thermogravimetry; 2007.
25. ASTM D5805-00, Standard test method for rubber from synthetic sources-carbon black in masterbatches; 2009.
26. Sawyer L, Grubb DT, Meyers GF. Polymer microscopy, XIV. 3rd ed. New York: Springer: 2008. p. 540.
27. Thomas EL. Structure of crystalline polymers, Hall IH, editor. London: Elsevier-Applied Science; 1984. p. 79.
28. Hobbs SY. Plastic polymer science and technology. Bayal MD, editor. New York: Wiley-Interscience; 1982. p. 239.
29. Grubb DT. Developments crystalline polymers, Bassett DC, editor. London: Applied Science; 1982, p. 1.
30. Hayat MA. Positive staining for electron microscopy. New York: Van Nostrand Reinhold; 1975.
31. Hayat M. Principles and techniques of electron microscopy-biological applications. 3rd ed. Boca Raton: CRC Press; 1989.
32. Lewis PR, Knight DP, editors. Staining methods for sectioned material. Amsterdam: North Holland-American Elsevier; 1977.
33. Berrisford DJ, Bolm C, Sharpless KB. Ligand-accelerated catalysis. Angewandte Chemie International Edition. 1995;34:1059–70.
34. Sacher RE, Macaione DP, Singler RE, Thermal analysis and characterization of elastomers and carbon black filler rubber composites for army applications" Army materials and mechanics research center wateron, Massachutts, Final report # AMMRC TR 1985;85–4, http://www.stormingmedia.us/52/5280/A528061.html.
35. Eilhannkwon K, Castaldi MJ. Fundamental understanding of the thermal degradation mechanisms of waste tires and their air pollutant generation in a N2 atmosphere. Environ Sci Technol. 2009;43:5996–6002.
36. Williams PT, Besler B, Taylor DT. The batch pyrolysis of tire waste–fuel properties of the derived pyrolytic oil and overall plant economics. Proc Instn Mech Eng. 1993;207:55–63.
37. Kaminsky W, Tossler H. Olefins from wastes. Chem Tech. 1992;22:108–13.
38. Wey MY, Liou BH, Wu SY, Zhang CH. The autothermal pyrolysis of waste tires. J Air Waste Manage Assoc. 1995;45:855–63.